https://doi.org/10.48048/tis.2021.1431

Kinetics, Isotherms and Thermodynamic Studies on Removal of Divalent Copper using Mallet Flower Leaf Powder as Bio-Adsorbent

Devarapalli Venkata Padma[1,2] and Susarla Venkata Ananta Rama Sastry[2,*]

[1]*Department of Chemical Engineering, A.U.C.O.E (A), Visakhapatnam, India*
[2]*Department of Chemical Engineering, MVGR College of Engineering (A), Vizianagaram, India*

([*]Corresponding author's e-mail: svarsastry@yahoo.com)

Received: 16 July 2020, Revised: 23 May 2021, Accepted: 16 June 2021

Abstract

The effectiveness and efficacy of Mallet Flower Leaf Powder (MFLP) as a bio-sorbent for the removal of heavy metal copper ions from the aqueous solutions have been studied. Experiments were conducted varying the pH, agitation time, temperature, biosorbent size and dosage as parameters. Speed of the mixing is kept at 200 rpm. The analysis of copper was done by using Atomic Absorption Spectrophotometer (AAS). The adsorption of copper was found to be dependent on pH and a maximum removal of 98.78 % was obtained at an optimum pH of 6.0. The optimum biosorbent dosage was 1 g for an agitation time of 40 min. The biosorption data obtained were validated for the best isotherm. The data collected were verified with the available adsorption isotherms. Experimental data obtained was well represented by Langmuir (R_L = 0.161, qm = 5.96 mg/g, R^2 = 0.9142), Freundlich (n = 0.64, K_f = 0.79L/g, R^2 = 0.9995) and Tempkin (R^2 = 0.9083, b_T = 267.63) isotherms, indicating favorable biosorption. The experimental data obtained were tested for the best fit and the Freundlich Model has yielded the best correlation with the highest regression coefficient, R^2 = 0.9844. Kinetic data has also been presented using thermodynamic analysis and the pseudo second order model was found to be the best fit with a correlation coefficient of 0.999. For the removal of copper from the solution, bioadsorbent showed a maximum adsorption capacity of 5.96 mg/g.

Keywords: Biosorption, Copper, FTIR, Heavy metals, Mallet Flower Leaf Powder (MFLP)

Introduction

The industries are responsible for the contamination of water resources. Conventional methods like precipitation, reduction, reverse osmosis, ion exchange, evaporation, and electro dialysis are economically viable for a high concentration of copper in wastewater [1-3]. When the concentration is low then adsorption is the only method that is economically viable. Conventional adsorbents such as Zeolites, Activated carbon, Activated alumina, Silica gel, Activated clay, Fullers' earth, Bone char, Alginates, etc. have been used to remove copper from wastewater. However, due to the high cost of these adsorbents and loss of activity during storage, regeneration and recycling; many investigators tried several low-cost adsorbents made from agricultural waste [4-6].

The present study is intended to remove Copper (II) from wastewater using low-cost adsorbent like Mallet Flower Leaf Powder (MLFP). The parameters covered are agitation time (t) adsorption dosage (l_a), pH, adsorbent particle size, (d_p) temperature (T), and initial concentration of Copper. The effect of these parameters on percentage removal (R_m) or recovery (R_c) and on metal uptake (q_e) is studied by conducting batch experiments.

Experiments were carried out to determine the adsorption capacity or the metal uptake 'q_e' of the MFLP adsorbent. Parameters studied were initial metal ion concentration of the experimental stock solutions, C_o; time of agitation; adsorbent particle size; temperature, and pH. The effect of these parameters on the removal of metal ions of Cu(II) was studied.

Materials and methods

Preparation of the adsorbent

The adsorbent was prepared using mallet flower leaf powder (*Scientific name: schefflera puccklerí*). The leaves are collected from the campus of MVGR College of Engineering (A), Vizianagaram, Andhra Pradesh, India. The leaves are washed with the tap water, sun dried, grinded using ultra-fine grinder and then screened through BSS meshes (100,150,240 mesh).

Batch mode adsorption studies

Batch experiments were carried out using 250 mL conical flasks. Stock solution was diluted with distilled water to make various concentrations of metal ions solutions varying from 20 - 100 ppm. The specific quantity of adsorbent (0.2 - 1.0 g) was added to the solution and agitated at 200 rpm in a rotary shaker for a predetermined period (5 - 90 min). The adsorbate was then decanted and separated from adsorbent using (Whatman no. 40) filter paper [7-9]. The clear solution was collected in sample bottles and stored for analysis using Atomic Absorption Spectrophotometer (AAS), model *Pinnacle-500.*

The percentage removal of Copper is calculated from Eq. (1);

$$(Co - Ce)\ \text{x}\ 100/Co \tag{1}$$

where C_o and C_e (mg/L) are the initial concentration (before adsorption) and final concentration (after adsorption).

Batch mode desorption studies

Batch desorption studies were performed in order to find whether the copper adsorption on the studied adsorbent is reversible or not. It is seen that the copper adsorption process is irreversible [10-12].

Results and discussions

Characterization of MFLP

Scanning electron microscopy (SEM) analysis

SEM images of MFLP before Copper adsorption are shown in **Figures 1(a) - 1(d)**. SEM showed the morphology and surface texture of MFLP at different magnifications. The adsorbent surface morphology revealed porous and zig-zag parts for the MFLP before adsorption and thus show the active sites [13-15].

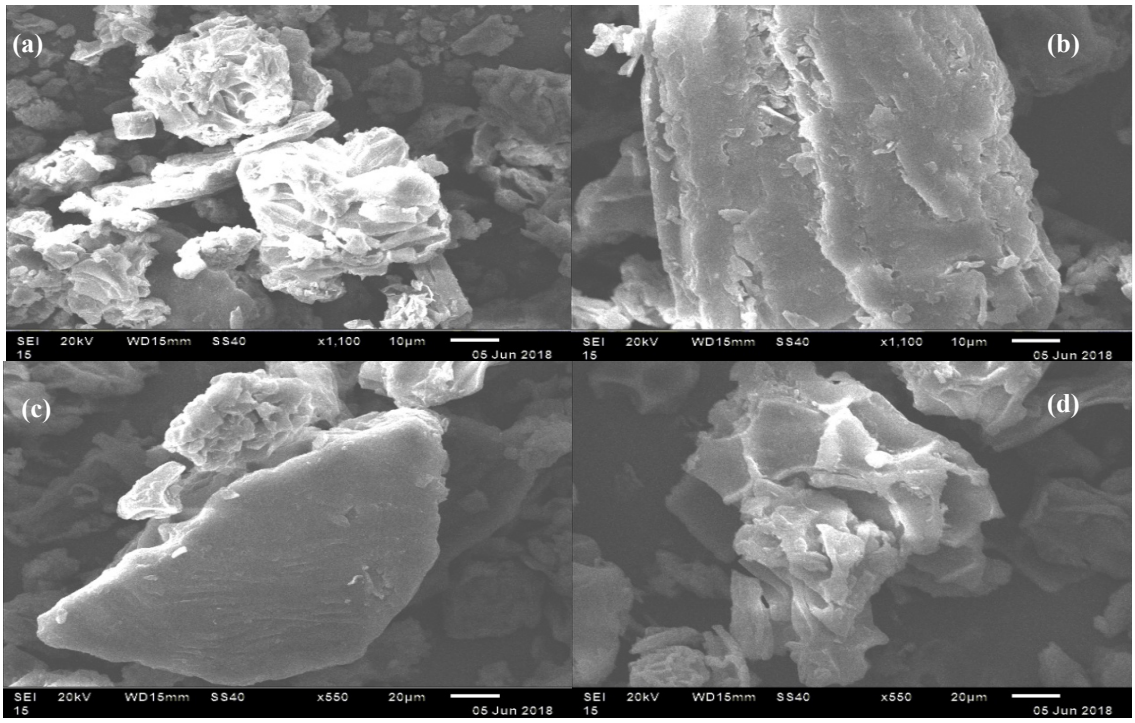

Figures 1(a) - 1(d) SEM micrographs of MFLP before adsorption of Copper.

SEM images of MFLP after Copper adsorption are shown in **Figure 1(e) - 1(h)**. The adsorbent surface morphology shows that the active sites were occupied by the metal ions after adsorption [22].

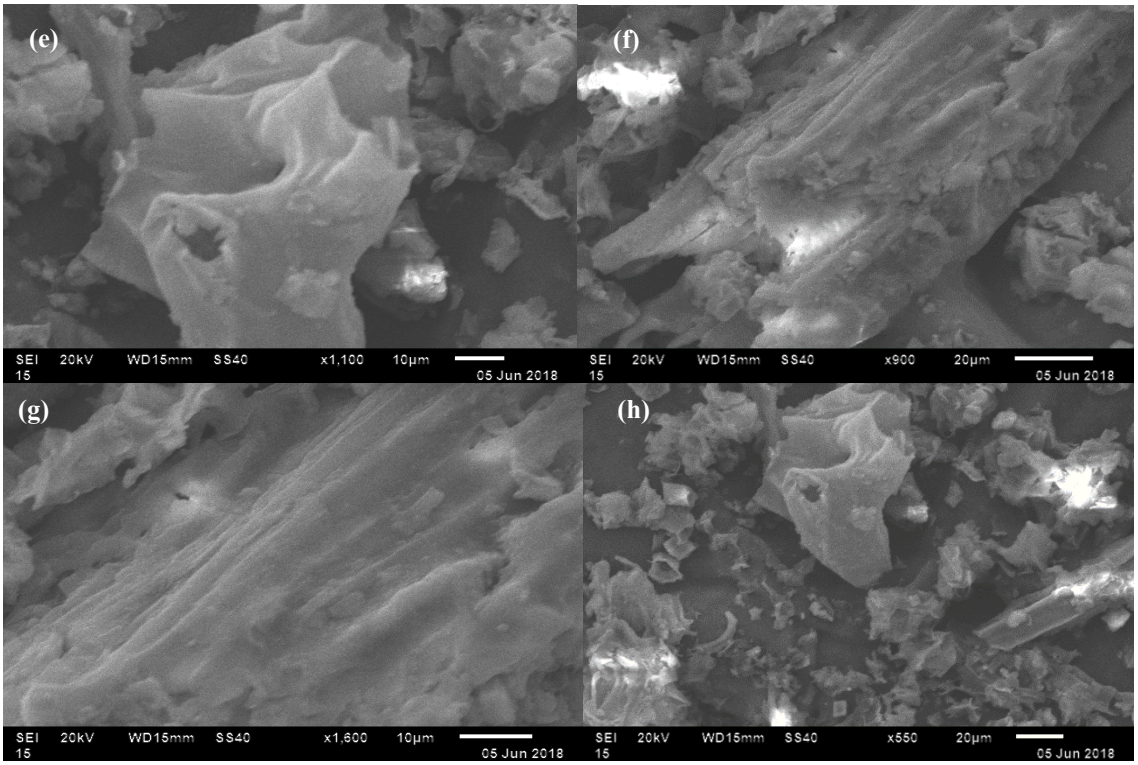

Figures 1(e) - 1(h) SEM micrographs of MFLP after adsorption of Copper.

Fourier transform infrared (FTIR) analysis

The adsorbent was characterized by using FTIR. FTIR has been shown for characterization and identification of functional groups, to understand the chemical composition of the adsorbent, which is very important for the uptake of metal ions. FTIR of adsorbent before and after Copper adsorption is shown in **Figures 2(a) - 2(b)**.

The range of wave number for the FTIR spectrum is from 400 to 4000 cm^{-1}. The peak, located at 2150 cm^{-1} is the characteristic peak of carbonyl group. According to **Figure 2**, a broad band at 3420 cm^{-1} is due to -OH group stretching. It can be concluded that hydroxyl and carbonyl were the main components of the adsorbent. It also shows that after adsorbing Cu(II), the peaks at 2150 and 3420 cm^{-1} reduced. This indicated the surface functional groups of adsorbent could combine with Cu(II) intensively. These groups had been reported to enhance metal ions adsorption [16-18].

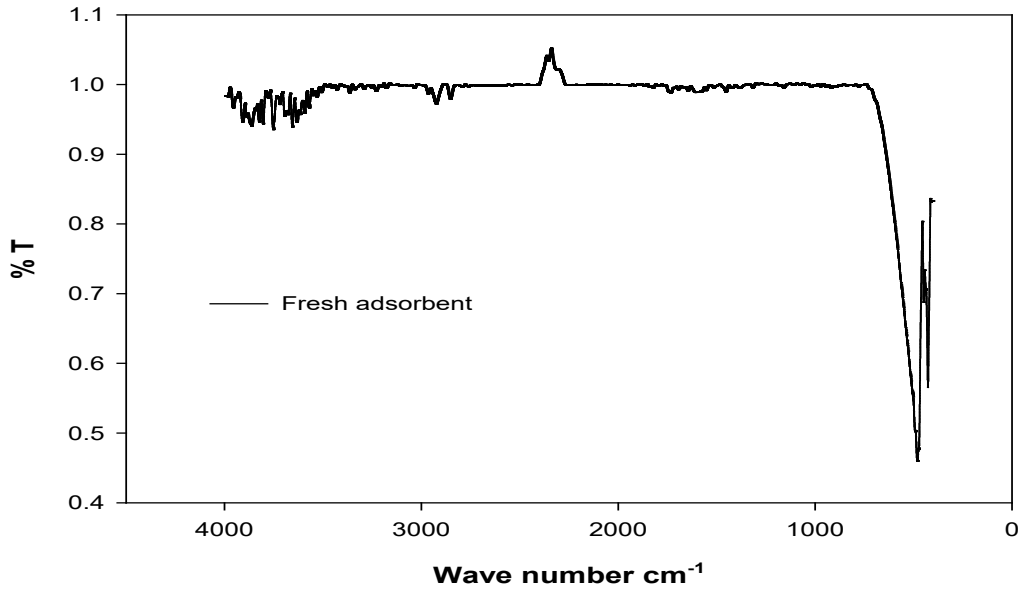

(a)

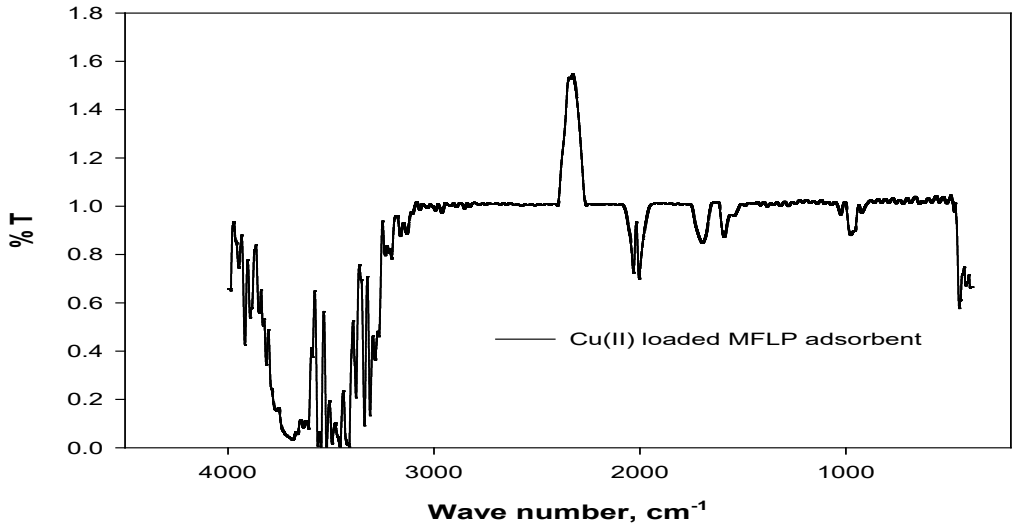

(b)

Figure 2 (a) FTIR image of pure adsorben and (b) FTIR image of Cu loaded adsorbent.

Effect of operating parameters on adsorption process

Different parameters are studied to evaluate the effect of adsorbent dosage, initial metal ion concentration, pH, contact time and temperature on removal of Copper using MFLP adsorbent (**Table 1**).

Table 1 Parameters studied for batch experimentation.

Parametric study	Metal ion concentration (ppm)	Adsorbent dosage (g)	Agitation time (min)	pH	Temperature (°C)	Adsorbent Size (microns)
Metal ion concentration	**20 - 100**	1	40	6	30	106
Adsorbent dosage	20	**0.2 - 1**	40	6	30	106
Agitation time	20	1	**5 - 90**	6	30	106
pH	20	1	40	**2 - 10**	30	106
Temperature	20	1	40	6	**10 - 50**	106
Adsorbent size	20	1	40	6	30	**74 - 149**

Effect of agitation time on adsorption

The data on percentage removal of copper were plotted against time is shown in **Figure 3** for different MFLP dosage values. The percent removal found to be very rapid in the initial 5 min and subsequently it is progressively raised to 40 min of agitation time. The percentage removal is nearly stable after 40 min. So, the equilibrium adsorption time for copper is observed to be 40 min [19-21].

The percentage removal has increased from 91.95 to 96.38 % in the time interval of 5 - 40 min. The percentage removal is higher initially, because of higher available surface area of the adsorbent and hence more surface adsorption sites, leading to better biosorption of copper. As the time proceeds, gradually the vacant active sites on adsorbent surface are fully occupied leaving no site for further adsorption. This results in equilibrium adsorption reaction between adsorbate, Cu(II) in solution and Cu(II) on adsorbent surface [22-24].

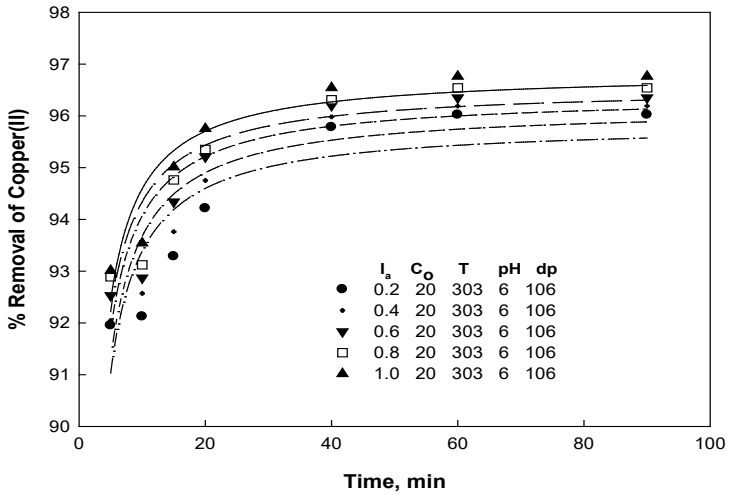

Figure 3 Effect of agitation time on adsorption of Cu (II).
[I_a-adsorbent dosage, C_o-Concentration, T-Temperature, dp-Adsorbent size]

Effect of initial concentration in aqueous solution

The effect of initial concentration of Cu(II) on the percentage removal of Cu(II) is shown through a graph in **Figure 4**. The percentage removal is slightly reduced from 98.78 to 98.5 by raising initial Cu(II) concentration (C_o) from 20 to 100 ppm [25-27]. At lower initial concentrations of Cu(II), adsorption was found to be a maximum of 98.78 %. For greater Cu(II) concentration, lesser percentage of Cu(II) was removed. Such performance is ascribed to the rise in the quantity of adsorbate to the fixed number of accessible active sites on adsorbent (as the quantity of adsorbent is kept constant) [22].

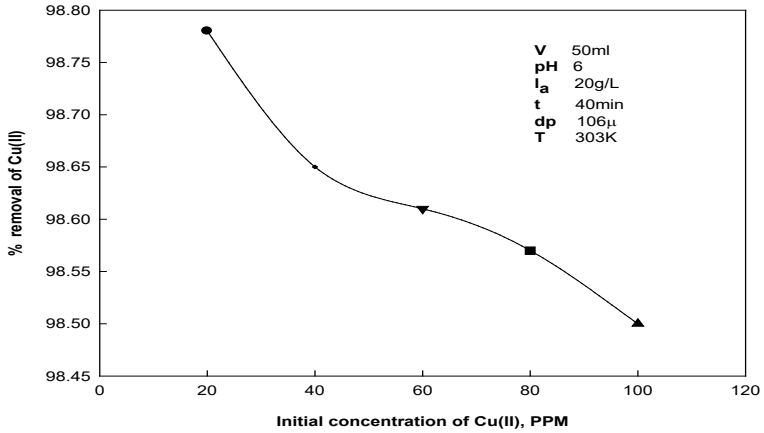

Figure 4 Effect of initial concentration in ppm on % recovery of Copper.

Effect of MFLP size on adsorption

The percentage removal of Cu(II) has progressively risen with decreasing size of adsorbent particles, as seen from the plots of **Figure 5**. The percentage removal increased from 85.49 to 97.1 as the adsorbent particle size decreased from 149 to 74 μ. This trend is expected as size of MFLP reduces, the surface area of MFLP obviously increases, and thereby a greater number of active sites on the adsorbent are better exposed to adsorbate [28-30].

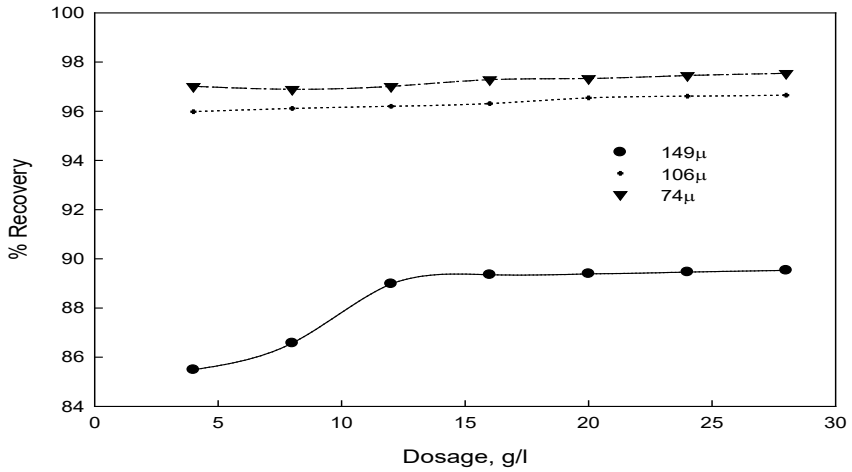

Figure 5 Effect of MFLP particle size on % removal of Cu(II).

Figure 5 signifies the difference in percentage removal of Cu(II) (pH = 6.0) against dosage of the adsorbent. The percentage removal was found to increase from 85.49 to 89.39 for particle size of 149 μ, while, for lower particle sizes there is no much variation in percentage removal when dosage is increased. As there is marginal (≤ 1 %) increase in the percentage removal when the particle size is decreased from 106 to 74 μ. Therefore, subsequent studies are carried out with 106 μ particle size as optimum particle size of adsorbent for Cu(II) removal.

Effect of solution pH on adsorption

To find the effect of pH on percentage removal of Copper, plots are shown in **Figure 6** for C_o values of all aqueous solutions at 303 K, 106 μ and 1 g adsorbent dosage. Considerable increase in percentage removal of Cu(II) is noticed as pH value is raised from 2 to 8. A maximum of percentage

removal of 98.78 was observed at a pH 6. Beyond pH 6, the values of percentage removal declined sharply for all initial sorbate solutions C_o. It was reported at lower pH values, the copper is present in different ionic forms in solution [31]. The active sites of adsorption surface of adsorbent tend to become positively charged and the negative radicals of Copper of the form $[Cu(OH)_3]^-$ have greater tendency to diffuse and adsorb on the positive adsorbent surface. While at higher pH values (above 6), conversion of copper to copper hydroxide is expected to be prevalent. The precipitated Copper loses its ability to adsorb on the adsorbent particle [32,33].

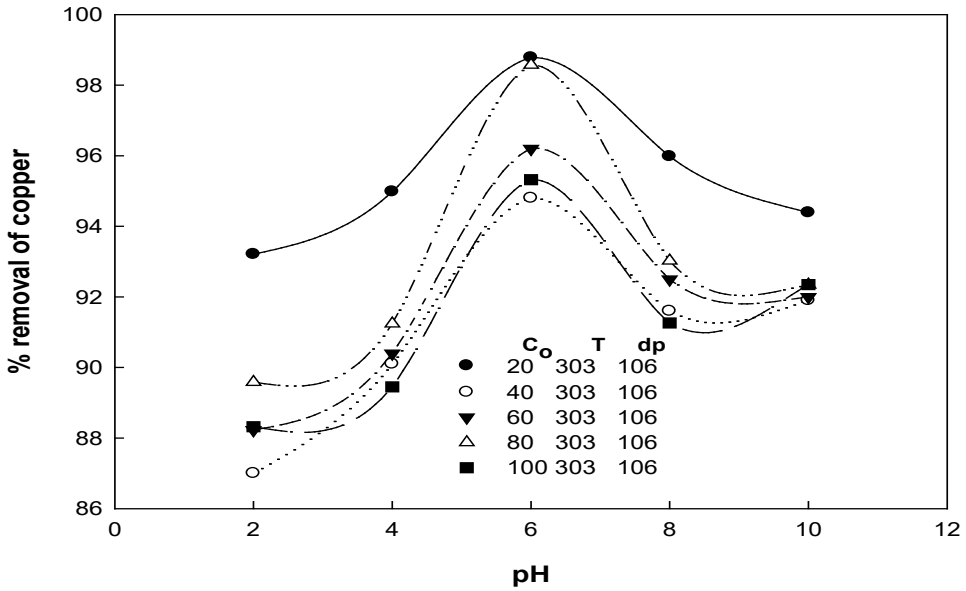

Figure 6 Effect of pH on adsorption of Cu(II).

Desorption studies

MFLP has good adsorption capacity. For this reason, it is necessary to find out the desorption characteristics of Cu(II) ions from MFLP. Experiments are conducted to investigate the desorption studies by proper treatment of the adsorbent without disturbing or damaging the structure either surface or internal structure of adsorbent. This would facilitate the re-use of adsorbent. The regeneration of the adsorbent renders any commercial adsorption process viable as fresh adsorbent need not be used [34-36].

The adsorbent after adsorption, is treated with suitable desorbents, normally acids or bases. In some cases, water also can be used as a successful desorbent.

The percentage of Cu(II) desorbed was determined by the Eq. (2);

$$\% \, Desorption = 100 \times \frac{V_D C_D}{q_e \, m} \quad (2)$$

where, C_D = concentration of and Cu(II) desorbed,
V_D = volume of desorbed solution,
m = mass of the adsorbed used for the study,
q_e = Ads capacity of the adsorbent (metal uptake).

The % desorption of Cr (II) indicates the suitability of MFLP as a good adsorbent.

Mechanism involved in desorption

Desorption is reverse of the adsorption, but the path of the desorption determines the percentage of removal. Metal loaded adsorbent, after reaching equilibrium, is treated with a given normality (known concentration) of NaOH/HCl for desorbing the metal ion. This is similar to solid-liquid leaching or extraction process.

As and when the metal loaded adsorbent is added to NaOH the concentration gradient between the sorbate on the adsorbent and sorbate in the desorbent initiates the desorption process. The basic nature of

the desorbent solution facilitates the detachment of sorbate metal ions. As the concentration of NaOH is increased by 2.5-fold, the percentage desorption increased significantly by about 40 - 45 %.

From the earlier adsorption studies, the data were found to fit well to Freundlich isotherm equation rather than Langmuir. This is suggestive that the adsorption of the sorbate on multilayer heterogenous surface is mostly favoured. In contrast, as Cu(II) absorption data showed a better fit to Langmuir isotherm equation, it is presumed that Cu(II) adsorption could have been caused on monolayer. 0.25 N desorbent (NaOH) showed a maximum percentage desorption of Cu was 55 %. The other parametric data were fixed at: pH 2, Temp 303 K, adsorbent dosage 1 g, time of duration 40 min and the solution contains 20 ppm Cu.

Experimental conditions for this case were: pH 6, temperature 303 K, adsorbent dosage 1g, time duration 40 min and the solution contains 20 ppm Cu. The percentage desorption of Cu was 52 % at HCl concentration of 0. 25 N.

Adsorption isotherms

Langmuir adsorption isotherm

The adsorption data on (C_e /q_e) was plotted against C_e for Cu(II) and shown in **Figure 7**. The data on Cu(II) were found to fit well with Langmuir Isotherm equation and Eq. (3) was obtained from regression of the data (**Table 2**).

$$\frac{c_e}{q_e} = 0.103C_e + 0.985 \quad (3)$$

$$q_m = 9.62\frac{mg}{g} \text{ and } R_L = 0.3216,\ R^2 = 0.818$$

The separation factor R, less than one indicates favorable biosorption, fulfilling Langmuir isotherm condition of $0 < R_L < 1$. The linear regression plots at all temperatures are shown in **Figure 8**.

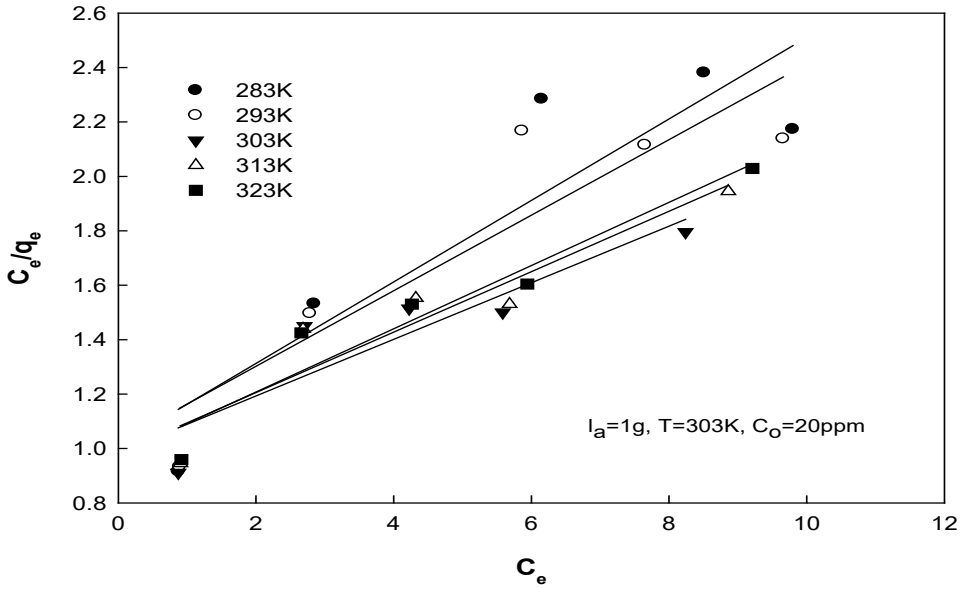

Figure 7 Langmuir isotherm for Cu(II).

Table 2 Langmuir isotherm and its coefficients for Cu(II).

S. No	Temperature (K)	Isotherm Equations	q_{max}(mg/g)	b	R_L	R^2
1	283	$\frac{C_e}{q_e} = 0.1497C_e + 1.013$	6.680027	0.147779	0.252808	0.814
2	293	$\frac{C_e}{q_e} = 0.1387C_e + 1.024$	7.209805	0.135449	0.269616	0.820
3	303	$\frac{C_e}{q_e} = 0.1039C_e + 0.985$	9.624639	0.105482	0.32158	0.818
4	313	$\frac{C_e}{q_e} = 0.111C_e + 0.983$	9.009009	0.11292	0.3069	0.883
5	323	$\frac{C_e}{q_e} = 0.1161C_e + 0.975$	8.613264	0.119077	0.295723	0.975

Freundlich isotherm

Similar analysis was made for the data on Cu(II) from the plotted data (**Figure 8**) in accordance with Freundlich isotherm equation. The results obtained are shown in **Table 3**.

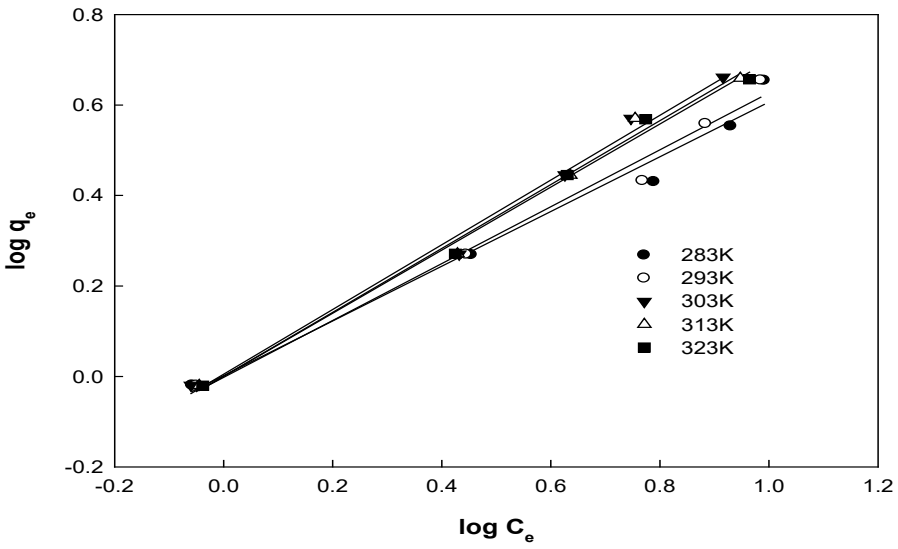

Figure 8 Adsorption data on Cu(II) in accordance with Freundlich Isotherm.

Table 3 Freundlich isotherm constants and coefficients for Cu(II).

S. No	Temperature (K)	Isotherm Equation	K_f	n	R^2
1	283	$logq_e = 0.604logC_e + 0.0017$	1.004045	1.653986	0.98
2	293	$logq_e = 0.628logC_e - 0.002$	0.995356	1.590837	0.985
3	303	$logq_e = 0.715\,logC_e + 0.005$	1.011603	1.398601	0.988
4	313	$logq_e = 0.706logC_e + 0.0003$	1.000807	1.416431	0.9908
5	323	$logq_e = 0.697logC_e + 0.0001$	1.000414	1.43472	0.9938

Tempkin isotherm

Similar analysis of the data on the adsorption of Cu(II) yielded the following isotherms at different temperatures (**Figure 9**, **Table 4**).

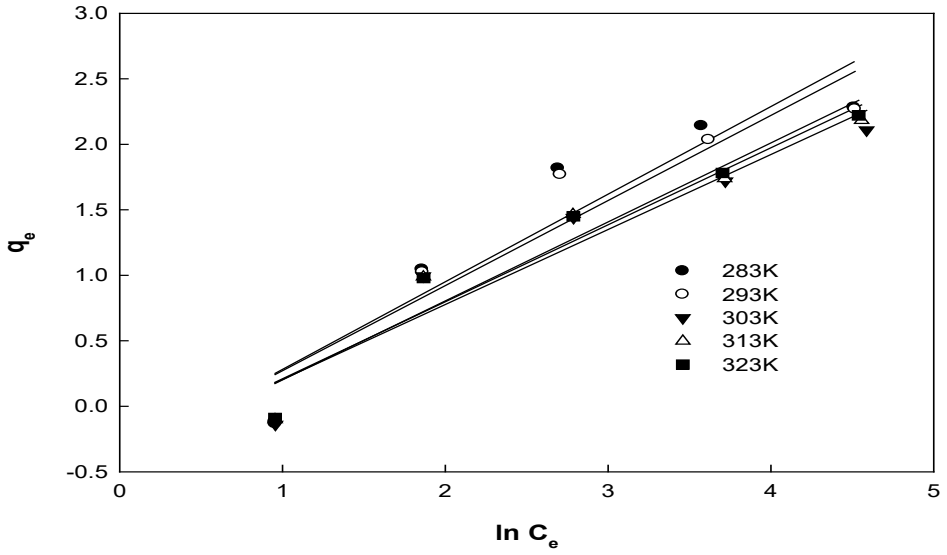

Figure 9 Temkin isotherm for Cu(II).

Table 4 Temkin isotherm constant and the regression data for copper.

S. No	Temperature (K)	Isotherm Equation	b_T	A_T(L/mg)	R^2
1	283	$logq_e = 0.669logC_e - 0.388$	3516.984	0.559915	0.877
2	293	$logq_e = 0.649\ logC_e - 0.378$	3751.158	0.558823	0.891
3	303	$logq_e = 0.572logC_e - 0.368$	4401.017	0.52567	0.913
4	313	$logq_e = 0.588\ logC_e - 0.379$	4425.65	0.525073	0.929
5	323	$logq_e = 0.603\ logC_e - 0.401$	4454.914	0.514156	0.9429

Adsorption kinetics

Pseudo first order model

The reaction rates of adsorbate-adsorbent system would provide good information for the design of a practical operating system to get better yield of removal/recovery of heavy metal ions either toxic or non-toxic from the effluent streams, within a given time constraint. Processing times can be optimized for quick and efficient removal or recovery processes. This information could be derived from the knowledge of the kinetics of reactions occurring between the adsorbent and adsorbate.

In view of the above, kinetic studies of adsorbent-adsorbate system of reactions have been carried out to arrive at a suitable mechanism of the reactions. Rates depicting the yields could be predicted from the different kinetic models provided, based on order of adsorbent-adsorbate reactions. Equilibrium data give the necessary drive for the transportation or diffusion of the solute (adsorbate) ions from solution to solid adsorbent surface. The kinetic studies could be modeled using the prevailing order within the given system.

Attempts are made to arrive at a suitable kinetic model for adsorption reactions between Cu, adsorbate and MFLP adsorbent. The diffusion rates of ions from solution to surface of adsorbent are probably monitored or controlled by a boundary. The rate kinetics in most of such instances follow pseudo first order rate equation of Lagergren given in Eq. (4);

$$\frac{dq_t}{dt} = k_{ad}(q_e - q_t) \quad (4)$$

where q_e and q_t are amount adsorbed at t (min) and equilibrium,
K_{ad} is rate constant of pseudo first order adsorption process.

The above equation can be written as Eq. (5);

$$\log(q_e - q_t) = \log q_e - \left(\frac{k_1}{2.303}\right)t \quad (5)$$

Plot of 'log (q_e–q_t)' vs. 't' gives straight line for the first order kinetics, making possible the calculation of first order rate constant (K_{ad}) for the adsorption process.

The above equation may not represent the experimental data due to the following 2 reasons;

1) K_{ad} (q_e – q_t) doesn't signify no. of accessible adsorption sites.
2) log q_e is not equivalent to intercept.

Pseudo second order model

If pseudo first order fails to fit in data, one can resort to the development of pseudo second order kinetic equation given as Eq. (6);

$$\frac{dq_t}{dt} = K_{ad}(q_e - q_t)^2 \quad (6)$$

where 'K' is the second order rate constant.

The above equation can be presented as Eq. (7);

$$\frac{t}{q_t} = \frac{1}{K_{ad}q_e^2} + \frac{1}{q_e}t \quad (7)$$

For the pseudo second order kinetics, the plot of (t/qt) versus t shown in **Figure 10** gives a linear equation, Eq. (8), facilitating the computation of qe and K [6].

$$\frac{t}{q} = 0.189t + 0.132 \quad (8)$$

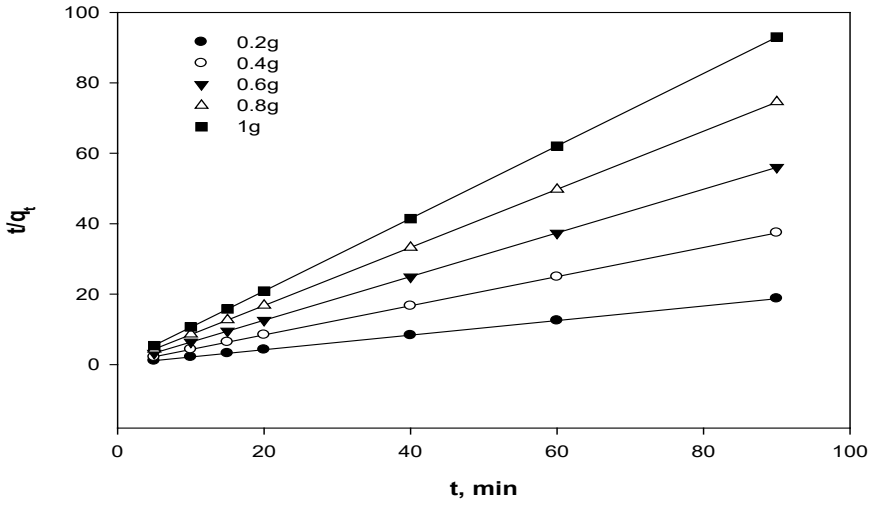

Figure 10 Psuedo second order kinetic model for Cu(II).

The data on t /q (metal uptake and time (agitation time) for Cu (II) with a particle size of 106 microns, 20 ppm solution, at a temperature of 303 K and pH = 6.0 are plotted for different adsorption dosages and shown in **Figure 10**. The calculated data qe_{cal}, qe_{exp}, R^2, Rate constant are shown in **Table 5**.

Table 5 Pseudo second order model constants and coefficients.

Kinetics	Parameters pH = 2, temperature	Model equation	qe_{cal}	qe_{exp}	R^2	Rate constant
2^{nd} order	0.2 g/50 mL 20 ppm	$\frac{t}{q} = 0.207t + 0.083$	4.830	4.7890	0.999	0.00355
	0.4 g/50 mL 20 ppm	$\frac{t}{q} = 0.413t + 0.150$	2.420	2.3995	0.999	0.02558
	0.6 g/50 mL 20ppm	$\frac{t}{q} = 0.620t + 0.196$	1.612	1.6033	0.999	0.07534
	0.8 g/50 mL 20 ppm	$\frac{t}{q} = 0.825t + 0.253$	1.212	1.2039	0.999	0.17219
	1 g/50 mL 20 ppm	$\frac{t}{q} = 1.030t + 0.300$	0.970	0.9654	0.999	0.31827

Diffusion model

The film diffusion, intra particle diffusion or interaction mechanisms might explain the rate determining step in the present adsorption reaction. To identify the exact mechanism for determining the rate determining step, the following Weber and Morris model [36] equation has been used.

Weber diffusion model Eq. (9);

$$q_t = K_{diff} t^{0.5} + C \quad (9)$$

The data on metal uptake is now plotted against √t for optimum adsorbent dosage of 80 ppm at 2 adsorbent dosages (**Table 6**). The data are shown segregated into 2 linear plots (A, B) of 2 different slopes. Plot A represents film diffusion while B represents intra-particle diffusion. The data are shown segregated into 2 linear curves with a distinct demarcation or break-up. This may be an indication that either film diffusion or intra-particle diffusion or together are controlling rate determining step. The plots A and B in **Figure 11**, however, show that film diffusion prevails predominantly.

where K_{diff} is the intra particle diffusion rate constant, mg/gm $min^{0.5}$

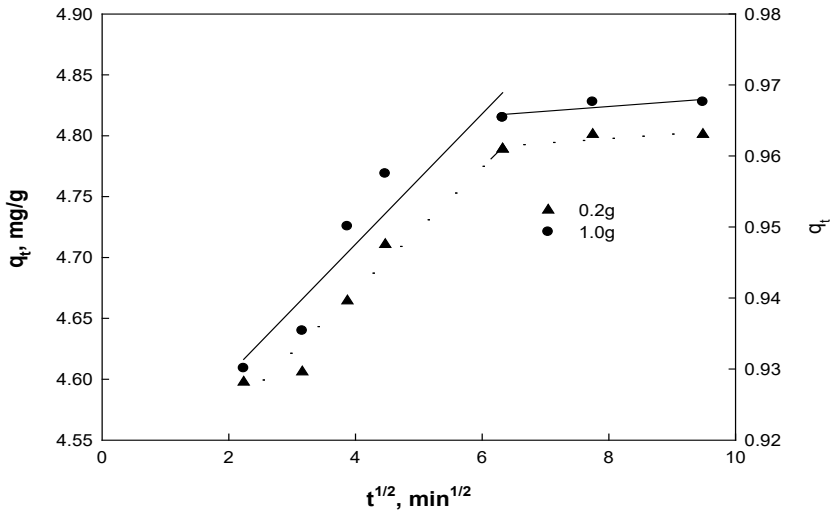

Figure 11 Intraparticle diffusion model for Cu(II).

Table 6 Intraparticle diffusion for Cu(II).

S. No	Dosage, g/L	Model equation	K_{diff}	Constant, C	R^2
1	0.2	$q_t = 0.0505t^{0.5} + 4.47$	0.0505	4.47	0.961
2	0.2	$q_t = 0.0036t^{0.5} + 4.76$	0.0036	4.76	0.698
3	1	$q_t = 0.0092t^{0.5} + 0.91$	0.0092	0.91	0.909
4	1	$q_t = 0.0006t^{0.5} + 0.96$	0.0006	0.96	0.698

Adsorption thermodynamics

The nature of heat interactions arise during adsorption between adsorbent and metal solution could be predicted from the thermodynamic data. These data can give us information whether the interactions are physical or chemical in nature. The study all through throw some light on the spontaneity of physical or chemical interactions [37,38]. In view of this, thermodynamic studies are carried out. The adsorbent - adsorbate interactions are established to be pseudo second order [29]. The change in augmentation of adsorption with temperature has been explained on the basis of Entropy change (ΔS), Enthalpy change (ΔH) and Gibbs free energy change (ΔG).

The equilibrium constant values K_D, for Cr (VI) on MFLP was calculated at different temperatures by using the Eqs. (10) - (12). These values were used to evaluate the thermodynamic parameters using the following equations;

$$K_D = C_{AE} / C_E \tag{10}$$

$$\Delta G = -RT \ln K_D \tag{11}$$

$$\ln k_D = \frac{\Delta S}{R} - \frac{\Delta H}{RT} \tag{12}$$

where, ΔG is the change in Gibbs free energy change (KJ/mol),
ΔH is the change in enthalpy change (KJ/mol),
ΔS is the change in entropy change (KJ/mol).

Sign of the ΔH value indicates the endothermic/exothermic nature of adsorption reaction.

1) ΔH (+ve) shows Endothermic reaction
2) ΔH (−ve) indicates Exothermic reaction

The data on rate constant, K_D calculated from pseudo-second order reaction equation (Eq. 12), were plotted against 1/T for all C_o values and shown in **Figure 12**. The slopes and intercepts of these plots would give us all the thermodynamic data on ΔH and ΔS from which ΔG can be calculated.

The data thus obtained for all the C_o values at different temperatures the thermo dynamic data are compiled and shown in **Table 7**.

The (−ve) values of ΔG are presented in table below that clearly indicates the spontaneity of reaction.

The (+ve) values for ΔH indicate the adsorption reaction is endothermic nature.

The +ve values of ΔH imply endothermic nature of adsorption and the values are +ve for C_o from 40 ppm to 100 ppm. However, for 20 ppm of Cu(II) solution the ΔH value was negative (−0.8 KJ/mole) indicating that adsorption for this specific instance and is exothermic in nature. The values of ΔH show how physical interactions are sufficiently strong for Copper (II) on MFLP adsorbent.

Gibbs free energy (ΔG)

The ΔG values of Cu(II) adsorption on MFLP under different temperatures were calculated using the equation;

$\Delta G = -RT \ln K_D$

Thermodynamic data for copper

The negative values of ΔG are presented in **Table 7**. The −ve values of ΔG imply spontaneous nature of adsorption. The ΔG values varied from −5104 to −8155 J/molK as its temperature varied from 283 to 323 K.

Entropy (ΔS): ΔS varied from 22 to 48 J/K mol.

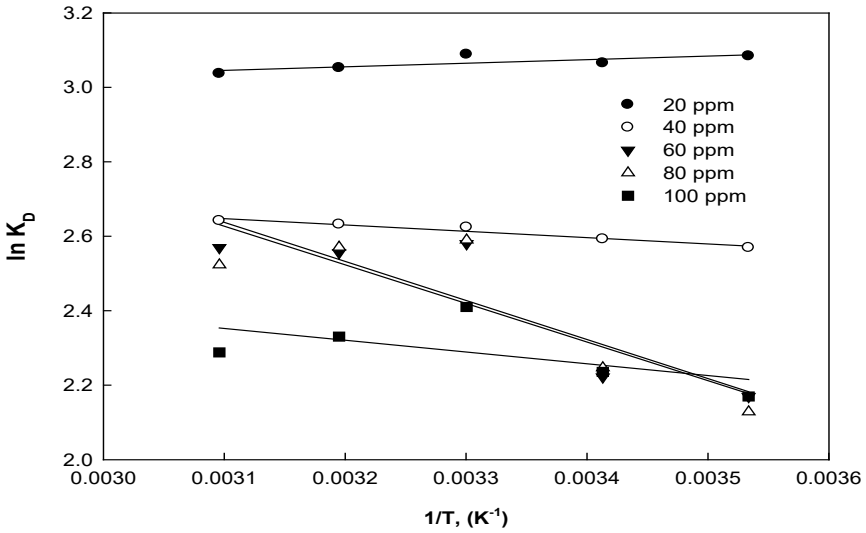

Figure 12 Thermodynamics plot for Cu(II).

Table 7 Thermodynamics data for copper and regression coefficients.

Initial concentration	Equation	ΔH, J/mole	ΔS, J/mole K	ΔG, J/mole				
ppm				283	293	303	313	323
20	$\ln K_D = -95.94\left(\frac{1}{T}\right) + 2.748$ $R^2 = 0.595$	−797.64	22.846	−7256.4	−6045.7	−5104.9	−5007.8	−5105.3
40	$\ln K_D = 169.73\left(\frac{1}{T}\right) + 3.17$ $R^2 = 0.95$	1411.14	26.355	−7467.6	−6316	−5413.8	−5473	−5446.4
60	$\ln K_D = 1049.43\left(\frac{1}{T}\right) + 5.89$ $R^2 = 0.782$	8724.96	48.969	−7780.7	−6610.7	−6500.3	−6524.3	−6071.8
80	$\ln K_D = 1037.42\left(\frac{1}{T}\right) + 5.84$ $R^2 = 0.728$	8625.11	48.553	−7944.1	−6849.4	−6651.6	−6689.3	−6065.1
100	$\ln K_D = 316.95\left(\frac{1}{T}\right) + 3.33$ $R^2 = 0.359$	2635.12	27.685	−8155.8	−7094.7	−6901.4	−6775.7	−6144.7

Conclusions

Experiments were carried out using Mallet Flower Leaf Powder. SEM and FTIR analysis showed the morphology and presence of active sites. The experimental data obtained was well represented by Langmuir (RL = 0.161, qm = 5.96 mg/g, R^2 = 0.9142), Freundlich (n = 0.64, Kf = 0.79 L/g, R^2 = 0.9995) and Tempkin (R^2 = 0.9083, bT = 267.63) isotherms, indicating favorable biosorption. Apart from this, thermodynamic studies were also well accepted for the removal of copper. The results suggested favorable removal efficiency of copper from waste water using MFLP. The maximum adsorption capacity of MFLP was found to be 5.96 mg of Copper/ gm of MFLP.

Acknowledgement

The authors acknowledge the support of the management of MVGR College of Engineering (Autonomous) in conducting the research work leading to the award of PhD of the first author. The authors also wish to express gratitude to Prof. C. Baskara Sarma for his advice.

References

[1] AAS Al-Gheethi, I Norli, J Lalung, AM Azlan, ZAN Farehah and MOA Kadir. Biosorption of heavy metals and cephalexin from secondary effluents by tolerant bacteria. *J. Clean Tech. Environ. Pol.* 2014; **16**, 137-48.

[2] AH Sulaymon, AA Mohammed and TJ Al-Musawi. Competitive biosorption of lead, cadmium, copper, and arsenic ions using algae. *Int. J. Environ. Sci. Poll. Res.* 2013; **20**, 3011-23.

[3] A Witek-Krowiak. Application of beech sawdust for removal of heavy metals from water: Biosorption and desorption studies. *Eur. J. Wood Wood Prod.* 2013; **71**, 227-36.

[4] A Hussain, J Maitra and KA Khan. Development of biochar and chitosan blend for heavy metals uptake from synthetic and industrial wastewater. *J. App. Water Sci.* 2017; **7**, 4525-37.

[5] A Yazdani, M Sayadi and A Heidari. Green biosynthesis of palladium oxide nanoparticles using dictyota indica seaweed and its application for adsorption. *J. Water Environ. Nanotech.* 2018; **3**, 337-47.

[6] B Krishna and P Venkateswarlu. Influence of *Ficus religioso* leaf powder on biosorption of cobalt. *Indian J. Chem. Tech.* 2011; **18**, 381-90.

[7] A Celik and A Demirbas. Removal of heavy metal ions from aqueous solutions via adsorption onto modified lignin from pulping wastes. *Energ. Sourc.* 2005; **27**, 67-77.

[8] DS Malik, CK Jain and AK Yadav. Removal of heavy metals from emerging cellulosic low-cost adsorbents: A review. *J. App. Water Sci.* 2017; **7**, 2113-36.

[9] D Dutta, SK Roy, B Das and AK Talukdar. Removal of Cu(II) and Pb(II) from aqueous solutions using nanoporous materials. *J. Phy. Chem. A* 2018; **92**, 976-83.

[10] E Bazrafshan, L Mohammadi, AA Moghaddam and A HosseinMahvi. Heavy metals removal from aqueous environments by electrocoagulation process - a systematic review. *J. Environ. Health Sci. Eng.* 2015; **13**, 74-9.

[11] F Migahed, A Abdelrazak and G Fawzy. Batch and continuous removal of heavy metals from industrial effluents using microbial consortia. *Int. J. Environ. Sci. Tech.* 2017; **14**, 1169-80.

[12] H Gao, R Tayebee, MF Abdizadeh, E Mansouri, M Latifnia and Z Pourmojahed. The efficient biogeneration of Ag and NiO nanoparticles from VPLE and a study of the anti-diabetic properties of the extract. *RSC Adv.* 2020; **10**, 3005-12.

[13] H Rezaei. Biosorption of chromium by using *Spirulina sp*. *Arabian J. Chem.* 2016; **9**, 846-53.

[14] IH Ali and HA Alrafai. Kinetic, isotherm and thermodynamic studies on biosorption of chromium (VI) by using activated carbon from leaves of *Ficus nitida*. *Chem. Central J.* 2016; **10**, 36-42.

[15] KC Khulbe and T Matsuura. Removal of heavy metals and pollutants by membrane adsorption techniques. *J. App. Water Sci.* 2018; **8**, 19-27.

[16] RM Kakhki, R Tayebee, M Mohammadpour and F Ahsani. Fast and highly efficient removal of anionic organic dyes with a new Cu modified nanoclinoptilolite. *J. Inclusion Phenom. Macrocyclic Chem.* 2018; **91**, 133-9.

[17] M Athar, U Farooq, SZ Ali and M Salman. Insight into the binding of copper(II) by non-toxic biodegradable material (Oryzasativa): Effect of modification and interfering ions. *J. Clean Tech. Environ. Pol.* 2014; **16**, 579-90.

[18] MH Sayadi, N Salmani, A Heidari and MR Rezaei. Bio-synthesis of palladium nanoparticle using Spirulina platensis alga extract and its application as adsorbent. *Surface. Interfac.* 2018; **10**, 136-43.

[19] MH Sayadi, O Rashki and ES Shahri. Application of modified Spirulina platensis and *Chlorella vulgaris* powder on the adsorption of heavy metals from aqueous solutions. *J. Environ. Chem. Eng.* 2019; **7**, 103-69.

[20] N Prakash, M Soundarrajan, SA Vendan, PN Sudha and NG Renganathan. Contemplating the feasibility of vermiculate blended chitosan for heavy metal removal from simulated industrial wastewater. *J. App. Water Sci.* 2017; **7**, 4207-18.

[21] DV Padma and SVAR Sastry. Biosorption of hexavalent chromium using mallet flower leaves powder as adsorbent. *TEST Eng. Manag.* 2020; **83**, 15714-29.

[22] DV Padma and SVAR Sastry. Biosorption of divalent copper from aqueous solution using mallet flower leaves powder as adsorbent. *Int. J. Environ. Waste Manag.* 2021, https://doi.org/10.1504/IJEWM.2022.10036313.
[23] DV Padma and SVAR Sastry. Kinetic studies on simultaneous biosorption of divalent copper and hexavalent chromium using mallet flower leaf powder. *J. Water Environ. Nanotech.* 2020; **5**, 204-17.
[24] S Moulay and N Bensacia. Removal of heavy metals by homolytically functionalized poly (acrylic acid) with hydroquinone. *Int. J. Ind. Chem.* 2016; **7**, 369-89.
[25] SVAR Sastry. Green synthesis and characterization of silver nano particles. *J. Water Environ. Nanotech.* 2020; **5**, 81-91.
[26] SVAR Sastry and BS Rao. Studies on adsorption of Cu(II) using spent tea extract (STE) from industrial wastewater. *J. Fut. Eng. Tech*. 2016; **11**, 31-5.
[27] SVAR Sastry and BS Rao. Determination of adsorption kinetics for removal of copper from wastewater using Spent Tea Extract (STE). *J. Fut. Eng. Tech.* 2017; **12**, 27-32.
[28] SVAR Sastry, BS Rao and DV Padma. Studies on selective batch adsorption of Cu(II) and Cr(VI) from aqueous solution. *TEST Eng. Manag.* 2020; **83**, 6794-7.
[29] H Shekari, MH Sayadi, MR Rezaei and A Allahresani. Synthesis of nickel ferrite/titanium oxide magnetic nanocomposite and its use to remove hexavalent chromium from aqueous solutions. *Surface. Interfac.* 2017; **8**, 199-205.
[30] S Huang and G Lin. Biosorption of Hg(II) and Cu(II) by biomass of dried Sargassum fusiform in aquatic solution. *J. Environ. Health Sci. Eng.* 2015; **13**, 21-9.
[31] S Choudhary, V Goyal and S Singh. Removal of Copper(II) and Chromium(VI) from aqueous solution using sorghum roots (S. bicolor): A kinetic and thermodynamic study. *J. Clean Tech. Environ. Pol.* 2014; **17**, 1039-51.
[32] S Iram, R Shabbir, H Zafar and M Javaid. Biosorption and bioaccumulation of copper and lead by heavy metal resistant fungal isolates. *Arabian J. Sci. Eng.* 2015; **40**, 1867-73.
[33] R Tayebee. Acid-thermal activated nanobentonite as an economic industrial adsorbent for malachite green from aqueous solutions: Optimization, isotherm, and thermodynamic studies. *J. Water Environ. Nanotech.* 2018; **3**, 40-50.
[34] R Tayebeea and N Mollaniab. Bio-removal of carcinogenic Cr(VI) by whole cells and cell-free extracts of a new native and highly chromate-resistant *Enterobacter sp*. *Desalin. Water Treat.* 2018; **111**, 258-66.
[35] VE Pakade, TD Ntuli and AE Ofomaja. Biosorption of hexavalent chromium from aqueous solutions by Macadamia nutshell powder. *J. App. Water Sci.* 2017; **7**, 3015-30.
[36] WJ Weber, JC Morris and J Sanit. Kinetics of adsorption on carbon from solution. *J. Sanitary Eng. Div. Am. Soc. Civ. Eng.* 1963; **89**, 31-8.
[37] XW Ang, VS Sethu, JM Andresen and MS Kumar. Copper(II) ion removal from aqueous solutions using biosorption technology: Thermodynamic and SEM-EDX studies. *J. Clean Tech. Environ. Pol.* 2013; **15**, 401-7.
[38] Z Sfaksi, N Azzouz, AA Wahab. Removal of chromium from water by cork waste. *Arabian J. Chem.* 2014; **7**, 37-42.